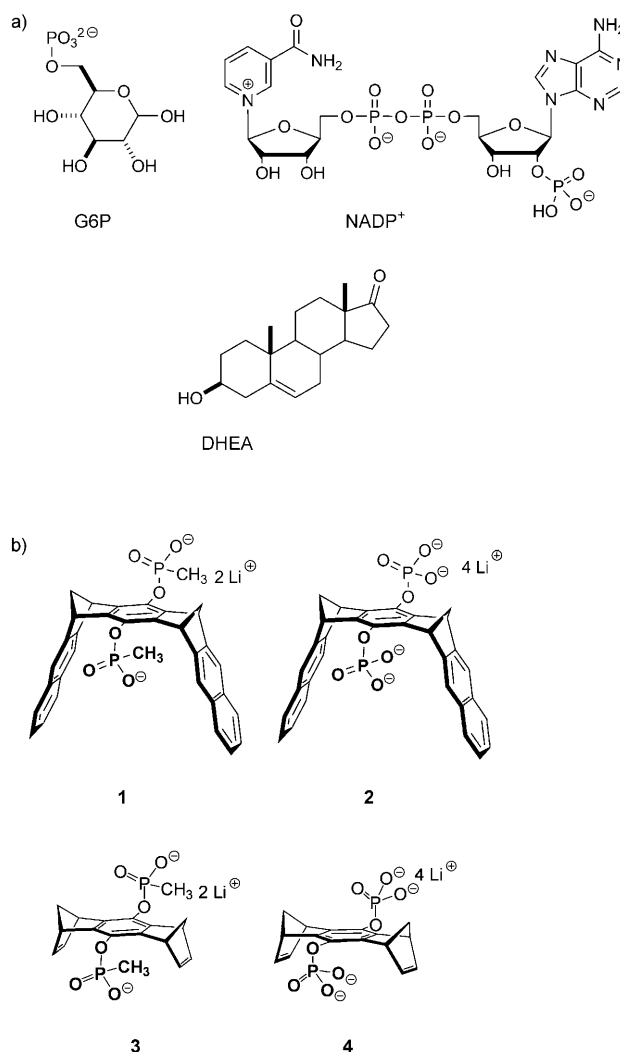


A Mechanism of Efficient G6PD Inhibition by a Molecular Clip**

Michael Kirsch, Peter Talbiersky, Jolanta Polkowska, Frank Bastkowski, Torsten Schaller, Herbert de Groot,* Frank-Gerrit Klärner,* and Thomas Schrader*

Glucose-6-phosphate dehydrogenase (G6PD) catalyzes the oxidation of glucose-6-phosphate to 6-phosphogluconate and the concomitant reduction of nicotinamide adenine dinucleotide phosphate (NADP⁺) to NADPH. This transformation is the first step in the pentose phosphate pathway.^[1] Critically lowered G6PD levels are the most common human enzyme deficiency in the world. This condition affects an estimated 400 million people and causes oxidative stress in red blood cells (erythrocytes),^[2] which ultimately results in neonatal jaundice and hemolytic anemia.^[3] Known inhibitors of G6PD^[4] include sugar phosphates and various nucleotides, which compete with the substrate or cofactor. However, some endogenous steroids are especially potent; the lead compound dehydroepiandrosterone (DHEA, Scheme 1)^[5] is thought to act as an uncompetitive inhibitor ($K_i = 9 \mu\text{M}$), most likely by binding to the ternary enzyme–coenzyme–substrate complex—a remarkable and very rare mechanism.^[6] The enzyme itself is only active in the dimeric state and is known to act according to the sequential, rapid-equilibrium, random model, without any preference for the order of substrate and cofactor docking.^[7] Analogue inhibitors will bind competitively with respect to either the substrate or the cofactor, as confirmed experimentally with thionicotinamide adenine dinucleotidephosphate (S-NADP⁺). With this compound, an IC_{50} value was observed that corresponded to approximately 50% of the concentration of NADP⁺ in the competitive mode.^[8]

In a joint effort, the Schrader and Klärner research groups developed phosphonate- and phosphate-substituted molecular clips (e.g., **1** and **2**, Scheme 1) that are able to recognize NAD(P)⁺ and pull its chemically active nicotinamide ring into their electron-rich cavity.^[9] These clips operate efficiently in an aqueous buffer by a combination of aromatic and Coulomb interactions if alkyl ammonium counterions are avoided and the pH value is kept close to neutral. The question arises whether these artificial host molecules can compete with



Scheme 1. a) Substrate (G6P), cofactor (NADP⁺), and steroid inhibitor (DHEA) of G6PD; b) new inhibitors for G6PD: clips **1** and **2**, and bridges **3** and **4**.

[*] Dipl.-Chem. P. Talbiersky, Dr. J. Polkowska, Dr. F. Bastkowski, Dr T. Schaller, Prof. Dr. F.-G. Klärner, Prof. Dr. T. Schrader
Institut für Organische Chemie, Universität Duisburg-Essen
Universitätsstrasse 5, 45117 Essen (Germany)
Fax: (+49) 201-183-4252
E-mail: frank.klaerner@uni-duisberg-essen.de
thomas.schrader@uni-due.de

Priv.-Doz. M. Kirsch, Prof. Dr. Dr. H. de Groot
Institut für Physiologische Chemie, Iniversitätsklinikum Essen,
Hufelandstrasse 55, 45122 Essen (Germany)
E-mail: herbert.de-groot@uni-duisberg-essen.de

[**] We are indebted to the DFG for financial support.

Supporting information for this article is available on the WWW under <http://dx.doi.org/10.1002/anie.200806175>.

dehydrogenases (e.g., G6PD) for NAD(P)⁺. Fluorescence and NMR spectroscopic titrations indicate that the enzyme G6PD ($K_d = 90 \mu\text{M}$; Ref. [10]: $45 \mu\text{M}$) and clips ($K_d = 200/250 \mu\text{M}$)^[11] both bind NADP⁺ in the high micromolar range (Table 1), so that a moderate influence of the clips on the enzymatic reaction can be expected.^[12,13]

For optimal performance, a large excess of the cofactor (200 μM) and the substrate (2 mM) is used in a classical G6PD assay (0.3 mM in the enzyme).^[14] Any efficient inhibitor that relies on cofactor capture must therefore furnish IC_{50} values in the same concentration range, as was the case in all initial

Table 1: Amount of cofactor necessary for the enzyme assay with various dehydrogenases in relation to the inhibitory activity of clips **1** and **2** and bridges **3** and **4**.

Enzyme ^[a]	Cofactor	Inhibitor	IC ₅₀ [μM]	IC ₅₀ /[cofactor]
ADH	NAD ⁺ (1800 μM)	clip 2	1500	0.8
GDH	NAD ⁺ (200 μM)	clip 1	> 1000	> 4.0
GDH	NAD ⁺ (200 μM)	clip 2	330 ± 25	1.5
GDH	NADP ⁺ (200 μM)	clip 2	255 ± 20	1.3
G6PD	NADP ⁺ (200 μM)	bridge 3	> 500	> 2.5
G6PD	NADP ⁺ (200 μM)	clip 1	350 ± 35	1.75
G6PD	NADP ⁺ (200 μM)	S-NADP ⁺	115 ± 5	0.58
G6PD	NADP ⁺ (200 μM)	bridge 4	53 ± 3	0.27
G6PD	NADP ⁺ (200 μM)	clip 2	7 ± 1	0.03
FDH	NAD ⁺ (1800 μM)	clip 2	43 ± 3	0.02
GAPDH	NAD ⁺ (400 μM)	clip 2	56 ± 2	0.14

[a] ADH = alcohol dehydrogenase, GDH = glucose dehydrogenase, G6PD = glucose-6-phosphate dehydrogenase, FDH = formate dehydrogenase, GAPDH = glyceraldehyde-3-phosphate dehydrogenase, NAD⁺ = nicotinamide adenine dinucleotide. The surprisingly high efficacy of clip **2** as enzyme inhibitor is highlighted in bold.

experiments with the phosphonate clip **1** (Table 1; IC₅₀ = 350 μM (equivalent to 1.8 equivalents of NADP⁺)). Subsequent kinetic analysis afforded a textbook example for competitive inhibition: The clip effectively competes with the Rossmann fold for NADP⁺ inclusion, and the enzyme can only be switched on by the external addition of large amounts of NADP⁺.^[15] This behavior points strongly to the postulated cofactor capture; it could also be confirmed for related redox enzymes (ADH,^[16] GDH) and seems to be a general new mechanism for moderate enzyme inhibition. However, when the related phosphate clip **2** was added under identical conditions to the G6PD assay instead of the phosphonate, the inhibitory effect was boosted into the far substoichiometric range (IC₅₀ = 7 μM, which is equivalent to 0.03 equivalents of NADP⁺), although both clips display a comparable affinity for NADP⁺.^[11] The origin of this unexpected shutdown mechanism was unclear at first, and a number of potential factors that might contribute to the observed strong inhibition were studied systematically (Table 1, Figure 1 b).

A first experimental hint came from a simple attempted ultrafiltration experiment (see Figure S5 in the Supporting Information), which indicated a high affinity of clip **2** for G6PD. This affinity was later confirmed quantitatively by isothermal titration calorimetry (ITC; K_d = 3 μM). By contrast, the very weak ITC binding curve for the phosphonate clip **1** with G6PD (K_d ≥ 1 mM) revealed an endothermic process, with no discrete structure for a putative enzyme/clip complex.

This remarkable divergence must hinge on the exchange of a negatively charged phosphate oxygen atom for a phosphonate methyl group. The 10–60-fold superior inhibition observed for the phosphate over the phosphonate of a given phosphate/phosphonate pair (**1/2** or **3/4**) serves as experimental evidence for essential electrostatic contributions in the binding event and possibly also for severe steric constraints (methyl versus O[−], Table 1). Interestingly, even a truncated version of the clip, **4**, which lacks the naphthalene side walls, operates substoichiometrically with respect to the cofactor: A sterically well-defined enzyme-binding site must

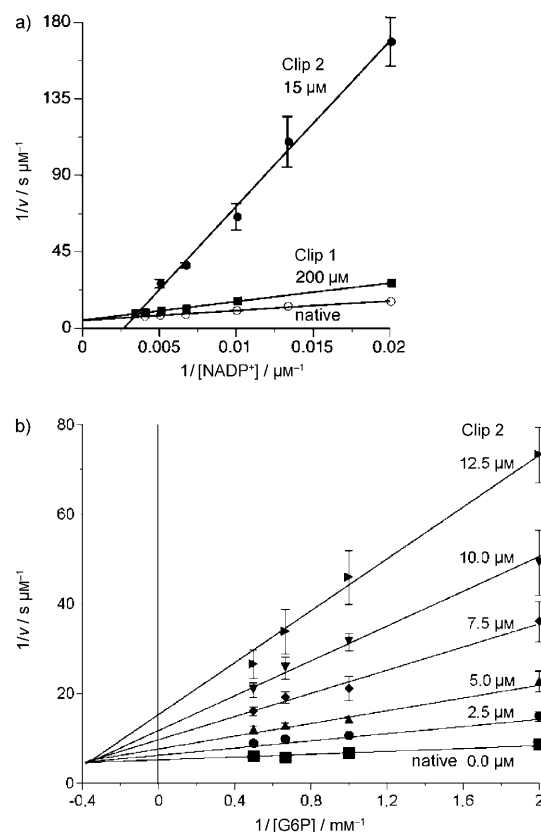


Figure 1. Enzyme kinetics with the clip inhibitor **2**, which interacts with the cofactor and the substrate. a) Conventional competitive (with clip **1**) and partial uncompetitive (with clip **2**) cofactor inhibition (v is the reaction rate). b) Mixed substrate inhibition.

exist that accommodates a phosphate anion preferably. Since both G6P and NADP⁺ carry phosphate anions, the clefts in which they bind are obvious candidates.

The enzyme interaction with clip **2** was compared to that with S-NADP⁺ (an NADP⁺-analogue inhibitor). As expected for a dehydrogenase operating according to the sequential, rapid-equilibrium, random model, enzyme inhibition by S-NADP⁺ is noncompetitive with respect to G6P as the variable substrate, but competitive with respect to the cofactor. In sharp contrast, clip **2** produces a very rare Lineweaver–Burk plot in which the native and inhibition curves intersect in the positive x,y quadrant (Figure 1 a). According to theoretical studies by Dixon and Webb and by Whiteley, the unusual slope found for clip **2** is characteristic of partial noncompetitive inhibition.^[17] Our tentative explanation assumes that the clip does “double duty” by binding to the enzyme/NADP⁺ complex and by somehow trapping the cofactor. The resulting ternary complex then acts as a much more powerful inhibitor, because it slows down the exchange of the otherwise loosely bound clip **2**.^[18] The assumed ternary complex is in a dynamic equilibrium with the free enzyme at all times, as evidenced by a switch-on experiment: The enzymatic activity of totally blocked G6PD (clip **2**: 15 μM) can be fully restored by adding NADP⁺ (1 mM; see Figure S4 in the Supporting Information).

To evaluate the importance of the structural features of the clips for their efficiency as inhibitors, we synthesized

truncated versions of the clips, **3** and **4**, which lack the aromatic naphthalene side walls.^[19] This simplification to leave the aromatic bridging unit was accompanied by a significant loss of inhibitory activity (approximately one order of magnitude; Table 1). Clearly, the side walls are indispensable—most likely for guest inclusion. The most significant gap occurs between the phosphate clip **2** and bridge **4**, an effect that might again point towards simultaneous interactions between the enzyme, clip, and cofactor. In this unusual ternary complex, the clip could act as a guest to the enzyme and at the same time host the cofactor.

A close inspection of the crystal structure of human G6PD reveals a binding groove equipped with a free arginine residue (Arg72) and other hydrogen-bond donors for the third NADP⁺ phosphate moiety.^[20] The virtual replacement of NADP⁺ with clip **2** gave a metastable complex structure with only one phosphate group bound inside the Rossmann fold (force-field calculation); however, after clip docking, the adenine moiety of the cofactor can slip into the open clip cavity, and its nicotinamide ring reaches down to the sugar substrate to produce a very stable complex and a perfect situation for partial inhibition. A subsequent molecular-dynamics (MD) simulation did not disrupt this putative complex even for half a nanosecond; on the contrary, small movements of several free lysine and arginine side chains led to new ion pairs with unpaired phosphate groups and greatly stabilized the ternary complex (Figure 2). Human G6PD contains two NADP⁺ molecules at distinctly different positions. One of these molecules is bound far away from the substrate, close to the dimerization interface, and has no direct influence on the catalytic activity.^[21] Since it is bound approximately 100 times more tightly than the catalytic cofactor ($K_d = 40$ nM), it cannot be replaced by clip **2** ($K_d = 3$ μ M).

The partial noncompetitive inhibition mechanism detailed above, however, is not sufficient to account for the observed total enzyme shut down. Detailed kinetic investigations finally revealed a second “mixed substrate inhibition” pathway, which suggests the replacement of bound G6P by clip **2**. Not only was a 2:1 stoichiometry found for clip/enzyme complexes by microcalorimetry, but a subsequent modeling experiment identified a second position at the bottom of the substrate-binding pocket that offered multiple favorable interactions with lysine, arginine, and aromatic residues (Figure 2). Thus, the clip does “triple duty”: As well as trapping NADP⁺, it occupies both the cofactor- and the substrate-binding site. It is the combination of the last two inhibition mechanisms that renders clip **2** so effective.^[22]

If this picture is correct, it should be possible to add the clip and cofactor sequentially in any order to G6PD and observe two favorable steps with a large enthalpy release corresponding to the successive formation of both inhibitory complexes. This hypothesis was confirmed by detailed microcalorimetric experiments, which provided strong evidence for the formation of the dual complex.^[23] The resulting thermodynamic picture for G6PD inhibition by clip **2** inside the substrate pocket and the Rossmann fold is depicted in Figure 3. The free enthalpy of formation of the ternary complex G6PD·2 × 2·NADP⁺ from the individual components

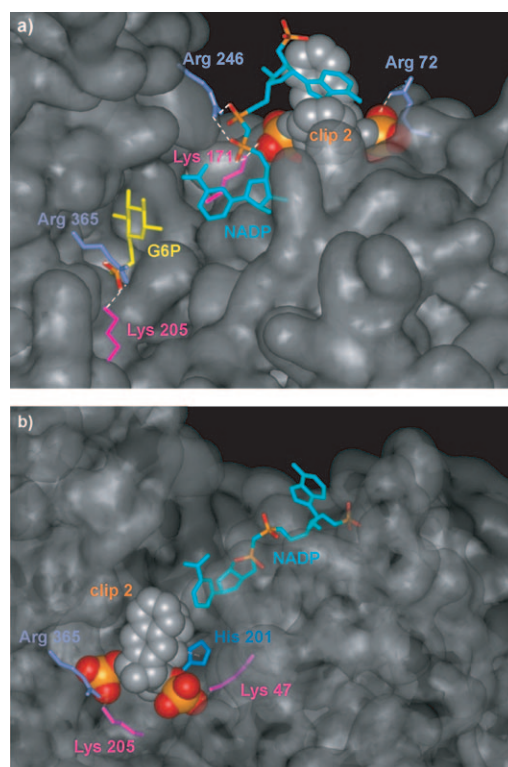


Figure 2. MD simulations illustrating the two modes of inhibition of G6PD by clip **2**. The simulations of a ternary (a) and a binary complex (b) were produced from parts of two PDB crystal structures (2BHL, 2BH9): a) virtual replacement of the cofactor with clip **2** and subsequent redocking of NADP⁺ inside the clip (MacroModel 8.0, water, OPLS-2005, 300 K, 0.6 ns); b) calculated enzyme complex with clip **2** occupying the substrate-binding site. Dotted white lines represent ion-pair-reinforced hydrogen bonds in strong salt bridges.

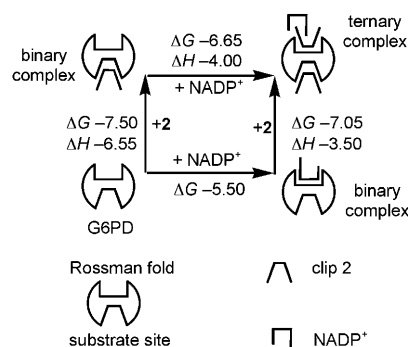


Figure 3. Thermodynamic scheme for successive complex formation between G6PD, clip **2**, and NADP⁺ (**2** and NADP⁺ both in excess) to explain the unusual and highly efficient inhibition kinetics; ΔH and ΔG values are in kcal mol⁻¹. The notation binary/ternary complex refers to the number of different molecular components and not to the stoichiometry of the complex.

was calculated from the thermodynamic data (listed in Figure 3) to be in good agreement for both pathways at -13 or -14 kcal mol⁻¹.

Intriguingly, other dehydrogenases, such as glucose dehydrogenase (GDH; NAD⁺- or NADP⁺-dependent), glycerinaldehyde-3-phosphate dehydrogenase (GAPDH), and alco-

hol dehydrogenase (ADH), do not show comparable inhibition levels. Clip **2** appears to be selective for G6PD. Apparently, the key is not clip-2-dependent NADP⁺ trapping, but most likely the specific combination of two inhibition pathways involving the concomitant formation of a binary and a ternary complex with one inhibitor molecule each.

Since G6PD is highly important for cell growth, clip **2** (like DHEA), if present in cells, would effectively decrease the proliferation rate of many cell types.^[24] The new clip might thus be used against endoscopically accessible tumors for local treatment. We therefore plan to develop membrane-permeable derivatives of **2** and optimize their affinity for G6PD.

Experimental Section

Synthesis of 4: Phosphoroxchloride (3.85 mmol) and triethylamine (0.72 mmol) were added to a stirred solution of the hydroquinone precursor^[19a] (0.27 mmol) in anhydrous THF (10 mL) at 0°C. Subsequent hydrolysis with water afforded the free bis(phosphoric acid), which was washed thoroughly and dried. Neutralization of the bis(phosphoric acid) with lithium hydroxide (1.09 mmol) in THF/water (v/v 1:1) gave the target compound. Purification over silica (elution with MeOH) afforded **4** (0.18 mmol, 67%) as a white solid. Decomposition: > 300°C; ¹H NMR (500 MHz, D₂O): δ = 2.15 (dt, 2H, ³J(11ⁱ-H, 11^a-H) = 6.9 Hz, ³J(11ⁱ-H, 6-H) = ³J(11ⁱ-H, 9-H) = 1.6 Hz, 11ⁱ-H, 12ⁱ-H), 2.21 (d(broad), 2H, 11^a-H, 12^a-H), 4.20–4.22 (m, 4H, 1-H, 4-H, 6-H, 9-H), 6.82 ppm (t, 4H, ³J(6-H, 7-H) = ⁴J(6-H, 8-H) = 2.0 Hz, 2-H, 3-H, 7-H, 8-H); positions of the protons of the methylene bridges are indicated by the letters i (inside, toward the center of the molecule) and a (away from the center of the molecule); ³¹P NMR (202 MHz, D₂O): δ = 0.77 ppm (s, OP(O)(O[−]Li⁺)₂); ¹³C NMR (126 MHz, D₂O): δ = 48.0 (d, C1, C4, C6, C9), 55.1–55.2 (m, OCH₃), 69.9 (t, C11, C12), 139.14 (m, C5, C10), 142.6 (m, C4a, C5a, C9a, C10a), 143.9 ppm (d, C2, C3, C7, C8); IR (KBr): $\tilde{\nu}$ = 3075 (C–H), 3001 (C–H), 2923 (C–H), 1464 (C–H), 707 cm^{−1} (C=C); UV/Vis (H₂O): λ_{max} (lg ϵ) = 214 (4.18), 254 (3.01); MS (ESI, MeOH): m/z : 198 [$M-4\text{Li}+2\text{H}$]²⁺, 419 [$M-4\text{Li}+2\text{H}+\text{Na}$][−]; HRMS: m/z calcd for C₁₆H₁₄NaO₈P₂: 419.007; found: 419.006.

NMR spectroscopic titrations: In the titration experiments, the total guest concentration [G]₀ was kept constant, whereas the total host concentration [H]₀ was varied: A defined amount of the receptor was dissolved in 0.6 mL of the solution containing the guest at a concentration [G]₀. The association constants K_a and the maximum complexation-induced ¹H NMR shifts, Δδ_{max}, were determined from the dependence of the guest ¹H NMR shifts, Δδ, on the host concentration by nonlinear regression analysis with the computer program TableCurve 2D, version 5.01.

Fluorescence titrations: G6PD, clip **1**, and clip **2** were excited at 280 nm in a fluorimeter, and their emission was monitored from 300 to 600 nm. In the host–guest experiment, which was conducted in sodium phosphate buffer (pH 7.6) in a quartz cuvette, the host solution (700 μL) was placed in the cuvette, and the guest solution was added a portion at a time. Changes in emission intensity were recorded and used in a standard nonlinear regression algorithm to calculate the appropriate association constants.

ITC measurements: ITC experiments were carried out with a Microcal VP-ITC instrument. Titrations were performed at 298 K with a reference power of 10 μcal s^{−1}. The host concentration in the cell was set at a value between 1 and 900 μM, and the guest was added with a syringe (0.1–17 mm) in 10 μL portions (5 μL for the first portion) over 8 s (4 s for the first addition). Single titration steps were spaced 360 s apart.

Enzyme assays: The activities of G6PD and other dehydrogenases were measured spectrophotometrically by following the initial,

linear increase in the absorbance at 340 nm of reaction mixtures containing potassium phosphate buffer (pH 7.6, 50 mM), the enzyme (0.3–3 nM), NAD(P)⁺ (200–1800 μM), the substrate (2–10 mM), MgCl₂ (1.4 mM), and a clip at various concentrations at 37°C. An optimized buffer was used to determine the IC₅₀ value of GAPDH: GAPDH (15 nM), AsO₄^{3−} (420 μM), PO₄^{3−} (5 mM), glyceraldehyde-3-phosphate (GAP; 1.6 mM), NAD⁺ (100–800 μM), NaHCO₃ (100 mM), pH 8.6, ethylenediaminetetraacetic acid (EDTA; 100 μM).^[25] For the determination of IC₅₀ values and the creation of Lineweaver–Burk plots, the reaction period was limited to 300 s to guarantee a strictly linear increase in the NAD(P)H concentration during the experiment. All experiments were initiated by adding the enzyme of interest.

Molecular modeling: The program MacroModel 8.0 was used for model building and as a graphical interface. For all energy minimizations and molecular-dynamics simulations (in aqueous solution), the built-in force field OPLS-2005 was chosen. The minimized structure, such as those shown in Figure 2, was used as the starting point for MD simulations. The temperature was maintained at 300 K, and the dynamics of the ternary complex were calculated for 1 ns, with 2000-step minimizations every 10 ps.

Full experimental data on fluorescence titrations, NMR spectroscopic titrations, and microcalorimetric titrations, inhibition experiments (determination of IC₅₀ values, Lineweaver–Burk plots), and the ultrafiltration experiment, as well as the kinetic enzyme model and NMR spectra of bridges **3** and **4**, can be found in the Supporting Information.

Received: December 18, 2008

Published online: March 12, 2009

Keywords: cofactors · enzymes · host–guest systems · inhibitors · molecular clips

- [1] a) M. Kotaka, S. Gover, L. Vandeputte-Rutten, S. W. N. Au, V. M. S. Lam, M. J. Adams, *Acta Crystallogr. Sect. D* **2005**, *61*, 495–504; b) H. R. Levy, *Biochem. Soc. Trans.* **1989**, *17*, 313–315.
- [2] S. Filosa, A. Fico, F. Paglialunga, M. Balestrieri, A. Crooke, P. Verde, P. Abrescia, J. M. Bautista, G. Martini, *Biochem. J.* **2003**, *370*, 935–943.
- [3] a) C. R. Scriver in *The Metabolic and Molecular Basis of Inherited Disease*, 7th ed., McGraw-Hill, **1995**, pp. 3367–3398; b) E. Beutler in *Hematology* (Eds.: W. J. Williams, E. Beutler, A. J. Erslev, M. A. Lichtman), McGraw-Hill, New York, **1990**, pp. 591–606.
- [4] Other known inhibitors of G6PD are isoflurane (difluoromethoxy-1-chloro-2,2,2-trifluoroethane), sevoflurane (1,1,1,3,3,3-hexafluoro-2-(fluoromethoxy)propane), diazepam (7-chloro-1-methyl-5-phenyl-1,3-dihydrobenzo[e][1,4]diazepin-2-one), and 6-aminonicotinamide.
- [5] G. Gordon, M. C. Mackow, H. R. Levy, *Arch. Biochem. Biophys.* **1995**, *318*, 25–29.
- [6] a) G. Gordon, J. Milne, N. Loveridge, *Arch. Biochem. Biophys.* **1995**, *318*, 25–29; b) G. W. Oertel, I. Rebele, *Biochim. Biophys. Acta Gen. Subj.* **1969**, *184*, 459–460.
- [7] a) K. B. Taylor, *Enzyme Kinetics and Mechanisms*, Kluwer Academic Publishers, Dordrecht, **2002**, chap. 6; b) X. T. Wang, S. W. N. Au, V. M. S. Lam, P. C. Engel, *Eur. J. Biochem.* **2002**, *269*, 3417–3424; c) O. Ibraheem, I. O. Adewale, A. Afolayan, *J. Biochem. Mol. Biol.* **2005**, *38*, 584–590.
- [8] S-NADP⁺ contains a sulfur atom instead of an oxygen atom in the nicotine amide functionality and therefore acts as a competitive inhibitor for the cofactor.
- [9] a) C. Jasper, T. Schrader, J. Panitzky, F.-G. Klärner, *Angew. Chem.* **2002**, *114*, 1411–1415; *Angew. Chem. Int. Ed.* **2002**, *41*,

- 1355–1358; b) T. Schrader, M. Fokkens, F.-G. Klärner, J. Polkowska, F. Bastkowski, *J. Org. Chem.* **2005**, *70*, 10227–10237.
- [10] $K_d = 45 \mu\text{M}$: E. A. Zaitseva, E. S. Chukrai, O. M. Poltorak, *Vestn. Mosk. Univ. Khim.* **2000**, *41*, 127–129.
- [11] K_d values were determined by NMR and fluorescence spectroscopic titrations (see the Supporting Information).
- [12] a) Lower K_d values of $20 \mu\text{M}$ have been reported for G6PD from lamb kidney cortex: N. N. Ulusu, B. Trandogan, F. E. Tezcan, *Biochimie* **2005**, *87*, 187–190; b) for G6PD from baker's yeast, see: B. J. Gould, M. A. Goheer, *Biochem. J.* **1976**, *157*, 289–393. The substrate (G6P) affinity is approximately $50 \mu\text{M}$.
- [13] According to NMR spectroscopic titrations, the substrate glucose-6-phosphate does not bind to clip **2** (see the Supporting Information).
- [14] H. U. Bergmeyer, J. Bergmeyer, M. Grassl, *Methods of Enzymatic Analysis, Vol. II*, 3rd ed., Verlag Chemie, Weinheim, **1983**.
- [15] M. G. Rossmann, D. Moras, K. W. Olsen, *Nature* **1974**, *250*, 194–199.
- [16] P. Talbiersky, F. Bastkowski, F.-G. Klärner, T. Schrader, *J. Am. Chem. Soc.* **2008**, *130*, 9824–9828.
- [17] M. Dixon, E. C. Webb, *Enzymes*, Longman, London, **1979**, pp. 343–344; C. G. Whiteley, *Biochem. Educ.* **2000**, *28*, 144–147.
- [18] Admittedly, an inconsistency remains, because all curves in a modified evaluation in the form of a plot of $v/v_0 - v$ against $1/[\text{clip } 2]$ intersect the abscissa in the positive and not, as postulated, in the negative range. Furthermore, the steepest slope is observed for the highest NADP^+ concentrations, in contrast to the results of Whitely.^[17] On the other hand, the Whitely data were obtained with a simpler “one-substrate enzyme” (mevalonate diphosphate decarboxylase).
- [19] a) M. Fokkens, C. Jasper, T. Schrader, F. Koziol, C. Ochsenfeld, J. Polkowska, M. Lobert, B. Kahlert, F.-G. Klärner, *Chem. Eur. J.* **2005**, *11*, 477–494; b) J. Polkowska, F. Bastkowski, T. Schrader, F.-G. Klärner, J. Zienau, F. Koziol, C. Ochsenfeld, *J. Phys. Org. Chem.* **2009**, DOI: 10.1002/poc.1519.
- [20] M. Kotaka, S. Gover, L. Vandeputte-Rutten, S. W. Au, V. M. Lam, M. J. Adams, *Acta Crystallogr. Sect. D* **2005**, *61*, 495–504.
- [21] Recent experiments with the apoenzyme suggest that the function of this NADP^+ molecule is to maintain the long-term stability of the whole enzyme: X.-T. Wang, T. F. Chan, V. M. S. Lam, P. C. Engel, *Protein Sci.* **2008**, *17*, 1403–1411.
- [22] The noncompetitive contribution towards the observed “mixed substrate inhibition” is most likely explained by a conformational change in the G6P-binding pocket induced by formation of the ternary complex inside the opposing Rossmann fold.
- [23] Unfortunately, fluorescence measurements proved unreliable, as the emission intensity of the clip was increased on enzyme docking, but quenched by cofactor inclusion.
- [24] W.-N. Tian, L. D. Braunstein, J. Pang, K. M. Stuhlmeier, Q.-C. Xi, X. Tian, R. C. Stanton, *J. Biol. Chem.* **1998**, *273*, 10609–10617.
- [25] M. Kirsch, H. de Groot, *J. Pineal Res.* **2008**, *44*, 244–249.